Optimization of the lithium-ion cell electrolyte composition through the use of the LiTDI salt

L. Niedzicki[a,*], E. Karpierz[a], A. Bitner[a], M. Kasprzyk[a], G.Z. Zukowska[a], M. Marcinek[a,1], W. Wieczorek[a,1]

[a]Warsaw University of Technology, Faculty of Chemistry, Noakowskiego 3, 00664 Warsaw, Poland

Abstract

Optimization of electrolyte composition for future traction batteries is presented in this paper. Extensive systematic studies of electrochemical performance, material utility and subsequently cost are reported in order to obtain optimal combination. Lithium salt of TDI anion (4,5-dicyano-2-trifluoromethanoimidazole) is used due to its superior thermal stability (compared to other commercially available lithium salts), stability in case of moisture presence, electrochemical stability and possible material savings when used in electrolyte. Critical selection of solvent mixtures is made with respect to the price of components.

Conductivity dependence of salt concentration is shown. For all studied systems the increased conductivity region is observed in the salt low and broad concentration range of 0.3 to 0.8 mol kg^{-1}. The structural and rheological explanation of the mentioned feature is performed. Lithium cation transference numbers are measured for highly conductive samples and used as the secondary parameter in the optimization procedure. The highest values are recorded for the very low salt content: 0.31 mol kg^{-1} LiTDI in EC:DMC (1:2 weight ratio) (σ = 5.09 mS cm^{-1}, t_{Li+} = 0.622) and 0.4 mol kg^{-1} LiTDI in EC:DMC:DME (8:16:1 weight ratio) (σ = 6.17 mS cm^{-1}, t_{Li+} = 0.648) giving the opportunity to substantial material savings in batteries.

[*] Corresponding author, tel.: +48 22 234 7421; fax: +48 22 628 2741; email: lniedzicki@ch.pw.edu.pl

[1] ISE Member

1. Introduction

Currently, the main barrier for battery electric vehicle (BEV) development is the price of the energy source – the traction battery. This expense is often over 50% of the car manufacturing cost. Decreasing the price of the battery is the main aim for most manufacturers. On the other hand, lithium-ion batteries are the backbone of the clean energy industry (wind farms, EVs, etc.). The Li-ion battery market was worth $11 billion in 2010 and is expected to reach $43 billion in 7 years [1]. Li-ion traction battery market alone is already worth $2 billion and is estimated to reach $14.6 billion by 2017 [2]. The electrolyte price takes a big share of the cost of the components in the Li-ion cell - 14-23% (depending on cell size) of the cost of materials, most of which is lithium salt [3,4]. For use in any portable application, electrolytes have to be safe, inexpensive, work in a wide range of temperatures, be stable in a wide range of potentials (for use with a wide range of electrode materials) and have high ionic conductivity for a good high-rate cycleability [5,6]. Maximizing the lithium cation conductivity value for a high charge-discharge cycle yield is also desirable. Economizing the lithium salt usage is advantageous in order to obtain inexpensive batteries for electronic device and automotive market development. Up until now, $LiPF_6$ salt has been used almost exclusively by the battery industry for lithium-ion cell production, and 1 M concentration has been suggested as an optimum by all manufacturers and researchers [7,8]. Optimization has been done so far by finding the maximum ionic conductivity (σ). However, no information on what portion of the charge is transported by cations (anions) can be provided simply through conductivity measurements. On the other hand, information about the mobility of electrolyte components can be obtained from ion transference number measurements. Better energy utility in real live batteries is enabled through a high cation transference number. That is why lithium cation conductivity (σ_{Li+}) is a more application-wise parameter. σ_{Li+} values can be obtained by multiplying the total ionic conductivity and the lithium cation transference number of the electrolyte (t_{Li+}). The crucial change in the cost of salt could be gained through the introduction of new salts.

Herein, the optimization of ionic conductivity, transference numbers and material savings of electrolytes based on LiTDI salt (lithium 4,5-dicyano-2-(trifluoromethyl)imidazole) is proposed. The route of synthesis and the basic properties (including thermal and electrochemical stabilities) of this have been published elsewhere [9].

In order for solvent mixtures to be used as an electrolyte matrix, mixtures of high relative permittivity solvent and of low melting point solvent(s) were chosen. Due to the low

flash point or high volatility/high vapor pressure of most of the solvents, only the traditional ones used in batteries, i.e. organic carbonates [10] were employed. Due to the known incompatibility of propylene carbonate (PC) with graphite [11,12], it was not used. Ethyl methyl carbonate (EMC), vinyl carbonate (VC) and fluoroethylene carbonate (FEC) were also omitted due to their relatively high price. The choice range of solvent mixtures was narrowed by the aforementioned decisions. Consequently, the used mixtures were based solely on ethylene carbonate (EC) as a high relative permittivity solvent, and diethyl carbonate (DEC) and/or dimethyl carbonate (DMC). Mixtures comprising 1,2-dimethoxyethane (DME) were also included, as it is known for increasing the conductivity of electrolytes when added as the co-solvent. If necessary, DME could be added to mixtures, but only in small quantities, for its known issue to grow electrolyte interface [13,14].

As for the safety of the chosen lithium salt, LiTDI, it is thermally stable up to 250°C - far more than any solvent boiling point or stability of many other organic lithium salts. LiTDI is also electrochemically stable up to 4.6 V vs. (Li/Li$^+$) - far more than is needed for commercially available electroactive materials. It is also fully stable in the presence of moisture. Smaller amount of fluorine in the anion in comparison to LiPF$_6$ is an additional, environmental-friendly advantage. Higher transference numbers of LiTDI should provide higher charge-discharge cycle yield. That is especially beneficial for high-energy applications, such as EVs or grid energy storage. More information on LiTDI safety, stability and its basic parameters in pure solvents and solvent mixtures is available elsewhere [9,15,16].

The high ionic conductivity and lithium cation transference numbers as well as the investigation of the highly beneficial broad ionic conductivity plateau plots are the subject of this study.

2. Experimental

The chosen solvent ratios in mixtures were based on phase diagrams [17,18] and industrial practice. The following mixtures were employed as a result: EC:DEC (1:2 weight ratio), EC:DMC (1:2 weight ratio), EC:DEC:DMC (1:1:1 weight ratio), EC:DEC:DME (8:16:1 weight ratio) and EC:DMC:DME (8:16:1 weight ratio). In order to shorten the notation, these mixtures are hereafter referred to by their short names: 1EC:2DEC, 1EC:2DMC, 1EC:1DEC:1DMC, 8EC:16DEC:1DME and 8EC:16DMC:1DME, respectively (numbers mean weight ratio values). The first three mixtures are the most common in the battery industry and for 1EC:2DMC and 1EC:1DEC:1DMC, these ratios are more or less

eutectic points. The last two are variants of the first two with an addition of DME. As suggested in literature, DME content should not excess 10%, so less than half of this limit – 4% – was used. Thus, solvent mixtures were chosen according to the safety and price requirements for electrolytes.

Samples of electrolyte were prepared in an argon-filled glovebox with less than 1 ppm of moisture content. A full range of LiTDI concentration (0.1 mol kg^{-1} to maximum solubility) electrolyte samples was made. 1 mol kg^{-1} samples of LiPF$_6$ (Sigma-Aldrich, battery grade) in 1EC:2DMC and 1EC:1DEC:1DMC were also made for comparison (as an industrial standard).

Ionic conductivity measurements were performed using electrochemical impedance spectroscopy (EIS) at the temperature of 20°C. Electrolyte samples were put into a micro conductivity cell with cell constant values of 0.3-0.7 cm^{-1} calibrated with precision of 0.3%. Cells were then placed in a cryostat-thermostat system (Haake K75 with a DC50 temperature controller). All impedance measurements were carried out on the computer-interfaced multichannel potentiostat with frequency response analyzer option Bio-Logic Science Instruments VMP3 within 500 kHz-1 Hz frequency range with 10 points per decade and 5 mV A.C. signal amplitude. Measurements were repeated at least three times for each concentration for higher consistency. Samples for conductivity measurements were prepared in an argon-filled glovebox with less than 1 ppm of moisture content.

Lithium cation transference numbers (t_+) were calculated using the D.C. polarization method combined with the A.C. impedance method introduced by Bruce and Vincent [19]. Samples of electrolytes were sandwiched between two lithium metal electrodes in a Swagelok-type cell. Impedance spectroscopy measurements were performed on a VMP3 multichannel potentiostat (with a frequency response analyzer module) with an A.C. signal of 5 mV in 500 kHz to 100 mHz range with 10 points per decade. Impedance spectra were analyzed with the Equivalent-circuit 4.55 program [20], with the equivalent circuit of two parts connected in series: 1. electrolyte resistance (R_e) and 2. parallel combination of interfacial resistance (R_i) and the constant phase element connected with it. Polarization measurements were also executed on the VMP3 multichannel potentiostat. Polarization with a 20 mV potential difference was applied on each sample until the current reached steady-state (defined as a state where the current difference in the last 10 minutes is lower than 1% relatively). For instance, typical chronoamperometry lasts between 3 and 4 hours before the ending condition takes place. Typical Nyquist impedance plots (for 0.3 mol kg^{-1} LiTDI in 1EC:1DEC:1DMC) are shown on the Figure 1. Exemplary experimental data (for 0.3 mol kg^{-1}

LiTDI in 1EC:1DEC:1DMC) used for estimation of lithium cation transference number are shown in Table 1. All measurements took place at the temperature of 20°C. The lithium cation transference number was then calculated as:

$$t_+ = (I_s (\Delta V - R_0 I_0)) / (I_0 (\Delta V - R_s I_s))$$

where: ΔV - D.C. voltage applied; R_0 - initial interfacial layer resistance; R_s - steady-state interfacial layer resistance; I_0 - initial current; I_s - steady-state current.

The t_+ experiment for each measured composition was performed on three samples for a higher consistency of data. Samples were handled in an argon-filled glovebox with less than 1 ppm of moisture content, then sealed and measured while thermostated.
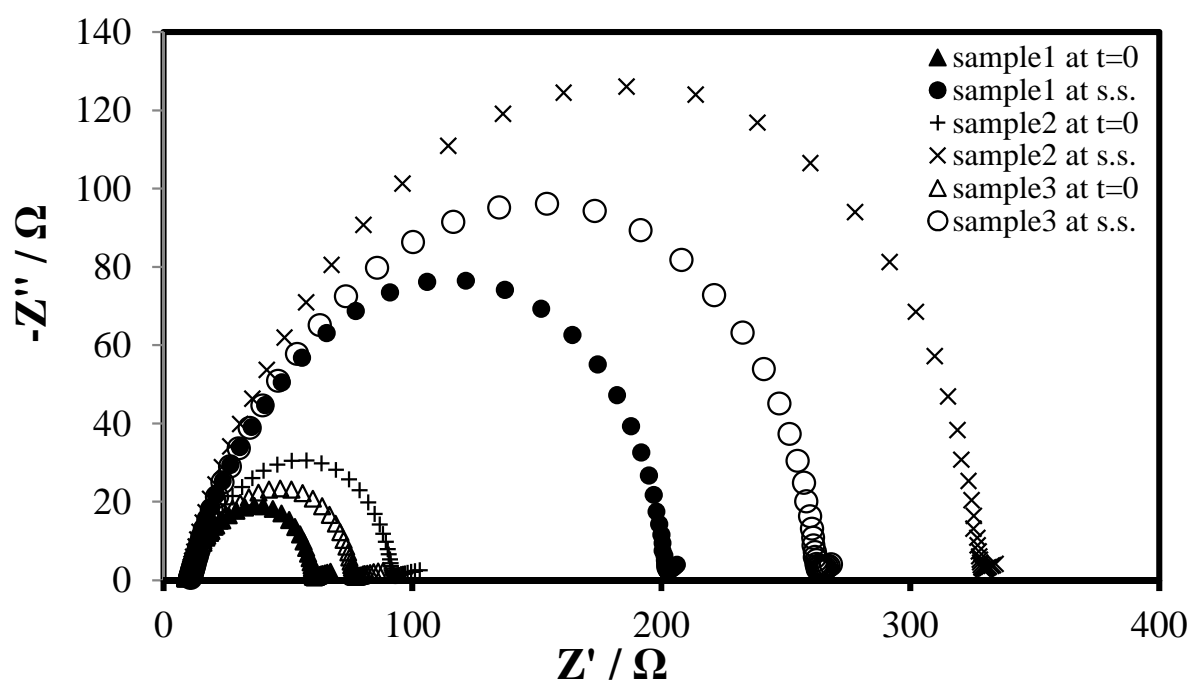

Fig. 1. Nyquist plots of Li | 0.3 mol kg-1 TDI in EC:DEC:DMC (1:1:1 weight ratio)| Li system measured for calculating interfacial resistance directly before polarization (t=0) and directly after polarization (s.s. – steady state). Interfacial resistance is used then for estimating lithium cation transference number.

	R_0 / Ω	R_s / Ω	I_0 / A	I_s / A	t_{Li+}
Sample 1	51.49	192.9	2.997×10^{-4}	8.385×10^{-5}	0.334
Sample 2	83.38	319.1	1.999×10^{-4}	5.393×10^{-5}	0.322
Sample 3	67.65	252.9	2.241×10^{-4}	6.330×10^{-5}	0.342

Table 1. Exemplary experimental data (for 0.3 mol kg^{-1} LiTDI in EC:DEC:DMC (1:1:1 weight ratio)) used for estimating lithium cation transference number.

Viscosity experiments were performed with a Physica MCR301 Anton Paar Rheometer with a CP40 cone plate and thermoelectric heat pump base for thermostating. Each time the 0.5 ml volume (excess) of the given electrolyte was used, it was thermostated with precision of 0.01°C at 20°C and measured in a shear rate of 10-1000 s^{-1}.

Infrared absorption spectra were recorded on a Perkin-Elmer System 2000 FT-IR spectrometer with a wavenumber resolution of 1 cm^{-1}. FT-IR studies were performed at room temperature. Spectra were obtained for samples in the form of a thin film sandwiched between two NaCl plates (salt concentration above 0.8 mol kg^{-1}) or placed in a cuvette with a 0.015 mm spacer (lower salt concentrations). Cuvettes were filled with solutions in a dry nitrogen-filled glovebox.

3. Results and discussion

The ionic conductivity dependence of LiTDI concentration in the investigated solvent mixtures is shown in Figure 2. All of the recorded curves have a similar shape, showing a broad plateau of high conductivity values. In Figure 2a, three mixtures of EC and DEC are shown to have this wide high-level conductivity range. In the case of 1EC:1DEC:1DMC mixture – the plateau onset takes place at 0.3 mol kg^{-1} and ends at 0.9 mol kg^{-1} with a small fluctuation in the course at 0.7 mol kg^{-1}. A similar shape occurs in another two conductivity plots. That is, for the 1EC:2DEC mixture, the onset takes place at 0.4 mol kg^{-1} (a sudden increase) and ends at 0.7 mol kg^{-1} (the global maximum). The 8EC:16DEC:1DME mixture has this plateau in the 0.3-1.3 mol kg^{-1} range, with the global maximum at 0.5 mol kg^{-1}.

The conductivity values of two other mixtures containing EC and DMC: 1EC:2DMC and 8EC:16DMC:1DME are shown in Figure 2b. Both mixtures have a similar high value range in the conductivity plot: with an onset at 0.3 and end after 0.7 mol kg^{-1}. An additional plateau occurs exclusively for the 8EC:16DMC:1DME mixture and takes place in the 0.9-1.3 mol kg^{-1} range. The global maxima are placed at 0.63 mol kg^{-1} for 1EC:2DMC and 0.4 mol kg^{-1} for 8EC:16DMC:1DME. A local maximum for the latter at 1 mol kg^{-1} also takes place at the beginning of the second high-value plateau on the conductivity plot.

For all these highly conductive samples (listed in the preceding paragraph), lithium cation transference numbers (t_{Li+}) were measured and lithium cation conductivities (σ_{Li+}) were calculated. The latter quantity is the product of ionic conductivity and the lithium cation transference number. The results, together with measurements and calculations for two LiPF$_6$
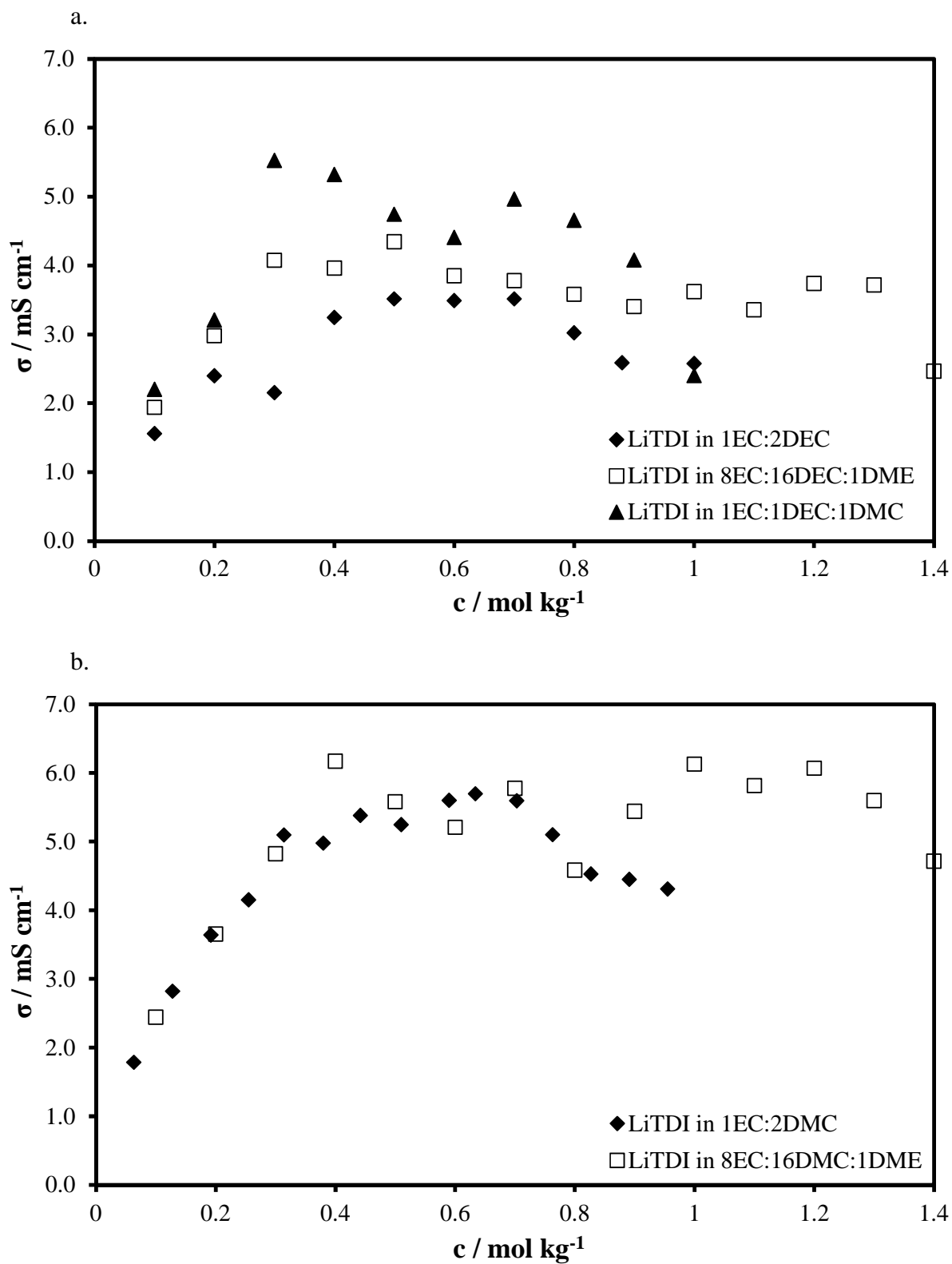
a.

b.

Fig. 2. Ionic conductivity dependence of LiTDI concentration in: a) EC:DEC (1:2 weight ratio), EC:DEC:DME (8:16:1 weight ratio) and EC:DEC:DMC (1:1:1 weight ratio) mixtures; b) EC:DMC (1:2 weight ratio) and EC:DMC:DME (8:16:1 weight ratio) mixtures.

contained samples for comparison, are summarized in Table 2. As can be seen, while $LiPF_6$ mixtures have higher ionic conductivity, after taking into account the lithium cation transference number, the real-performance parameter is obtained, which is low in the case of $LiPF_6$, due to very small t_{Li+} values. $LiPF_6$ in the 1EC:1DEC:1DMC mixture is surpassed that way by most of the presented LiTDI compositions, and the $LiPF_6$-1EC:2DMC mixture has a lower σ_{Li+} value than some LiTDI in the 8EC:16DEC:1DME and 8EC:16DMC:1DME compositions. Additionally, as it is worth mentioning, very high ionic conductivities and lithium cation conductivities were obtained for very low concentrations (0.31 mol kg^{-1} in the case of 1EC:2DMC, 0.4 mol kg^{-1} in 8EC:16DMC:1DME and 0.5 mol kg^{-1} in 8EC:16DEC:1DME), which is crucial for decreasing the overall cost of the lithium-ion cells' electrolyte.

Mixture	σ / mS cm^{-1}	T_{Li+} / -	σ_{Li+} / mS cm^{-1}
0.3 mol kg^{-1} LiTDI in EC:DEC:DMC (1:1:1)	5.52	0.333	1.84
0.7 mol kg^{-1} LiTDI in EC:DEC:DMC (1:1:1)	4.96	0.497	2.47
0.4 mol kg^{-1} LiTDI in EC:DEC (1:2)	3.24	0.601	1.95
0.7 mol kg^{-1} LiTDI in EC:DEC (1:2)	3.51	0.563	1.98
0.31 mol kg^{-1} LiTDI in EC:DMC (1:2)	5.09	0.622	3.17
0.63 mol kg^{-1} LiTDI in EC:DMC (1:2)	5.70	0.553	3.15
0.3 mol kg^{-1} LiTDI in EC:DEC:DME (8:16:1)	4.07	0.614	2.50
0.5 mol kg^{-1} LiTDI in EC:DEC:DME (8:16:1)	4.35	0.850	3.69
1.2 mol kg^{-1} LiTDI in EC:DEC:DME (8:16:1)	3.74	0.666	2.49
0.4 mol kg^{-1} LiTDI in EC:DMC:DME (8:16:1)	6.17	0.648	4.00
1.0 mol kg^{-1} LiTDI in EC:DMC:DME (8:16:1)	6.13	0.731	4.48
1.0 mol kg^{-1} $LiPF_6$ in EC:DEC:DMC (1:1:1)	10.08	0.244	2.46
1.0 mol kg^{-1} $LiPF_6$ in EC:DMC (1:2)	10.15	0.350	3.55

Table 2. Recommended compositions out of investigated electrolytes regarding materials savings and conductive parameters (numbers in parentheses mean weight ratio values).

For the explanation of the phenomenon of the wide high-value conductivity ranges along the salt concentration, an additional investigation of the described electrolytes was performed. Combining the viscosity curves for two exemplary mixtures (Figure 3) with the ionic conductivity plots led to an explanation of their unusual shapes. The rapid increases of initial conductivity are the result of a decrease (1EC:2DMC) or slow increase (8EC:16DMC:1DME) of viscosities in the 0.1-0.2 mol kg^{-1} range. The further plateau regions, or the stable high-value range of conductivity, also results from a plateau of viscosity (0.3-0.4
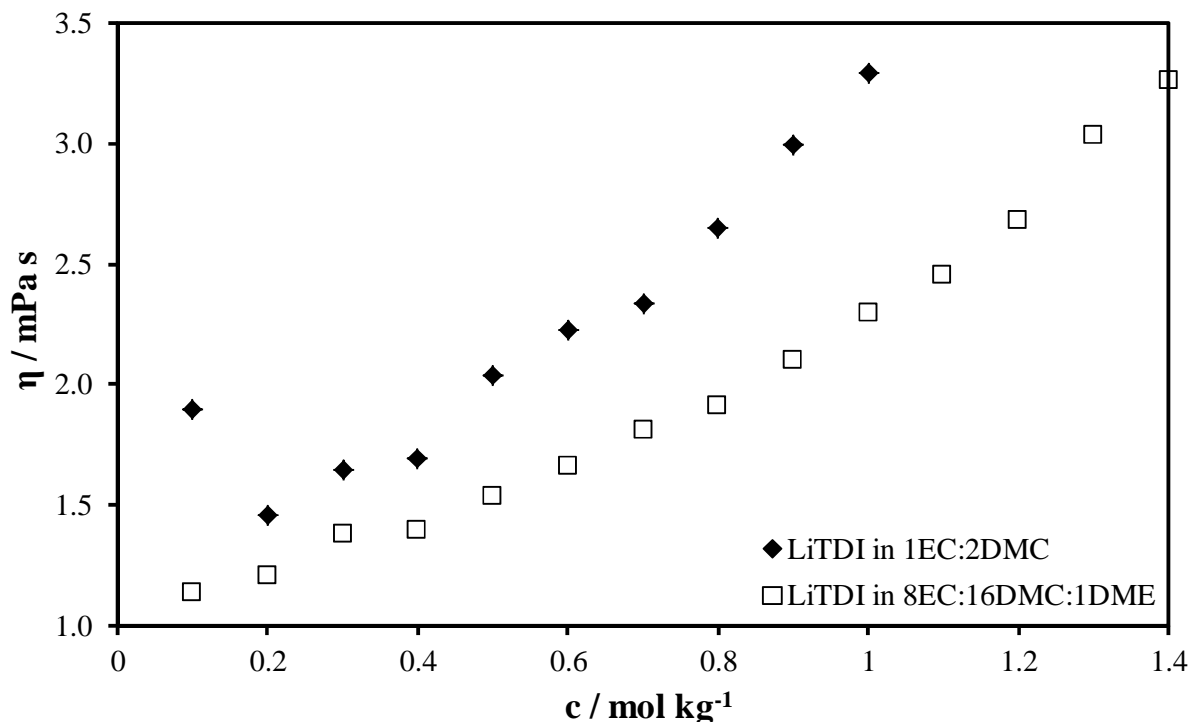
Fig. 3. Viscosity dependence of LiTDI concentration in EC:DMC (1:2 weight ratio) and EC:DMC:DME (8:16:1 weight ratio) mixtures.

mol kg^{-1} in both mixtures), as well local conductivity minima being joined with the region of dramatic increases in viscosity (0.5 and 0.8 mol kg^{-1} in both mixtures, 1.3 mol kg^{-1} in 8EC:16DMC:1DME). These kind of dependences can also be observed for other points: 0.6-0.7 mol kg^{-1} in 1EC:2DMC, 0.7-0.8 and 1.0-1.2 mol kg^{-1} in 8EC:16DMC:1DME. Such discrepancies in a viscosity plot, which usually tend to be monotonic and congruous, should be possible to explain by an investigation of solvation and association in those solutions.

The most useful tool to study or even quantitatively determine ionic aggregates is infrared spectroscopy. As it is known [21, 22], an increase in the salt concentration results in the formation of various types of ionic associates such as ionic pairs, triplets or dimers (pairs of ionic pairs). Due to the presence of several possible coordination sites in the TDI anion structure, free anions, neutral ionic pairs and also neutral dimers can be formed. Similarly, the solvation of cations by solvent molecules influences chemical bonds of the latter, which results in an alteration of the vibrational spectra. In the case of ethylene carbonate, the most suitable band for studying ionic association is the ring deformation vibration at 716 cm^{-1}, which, as the salt concentration increases, is accompanied by a second band at 729 cm^{-1}, attributed to lithium coordinated solvent. The fraction of associated and free (unassociated) EC molecules is shown in Figure 4. The fraction of the free EC decrease with the increase of
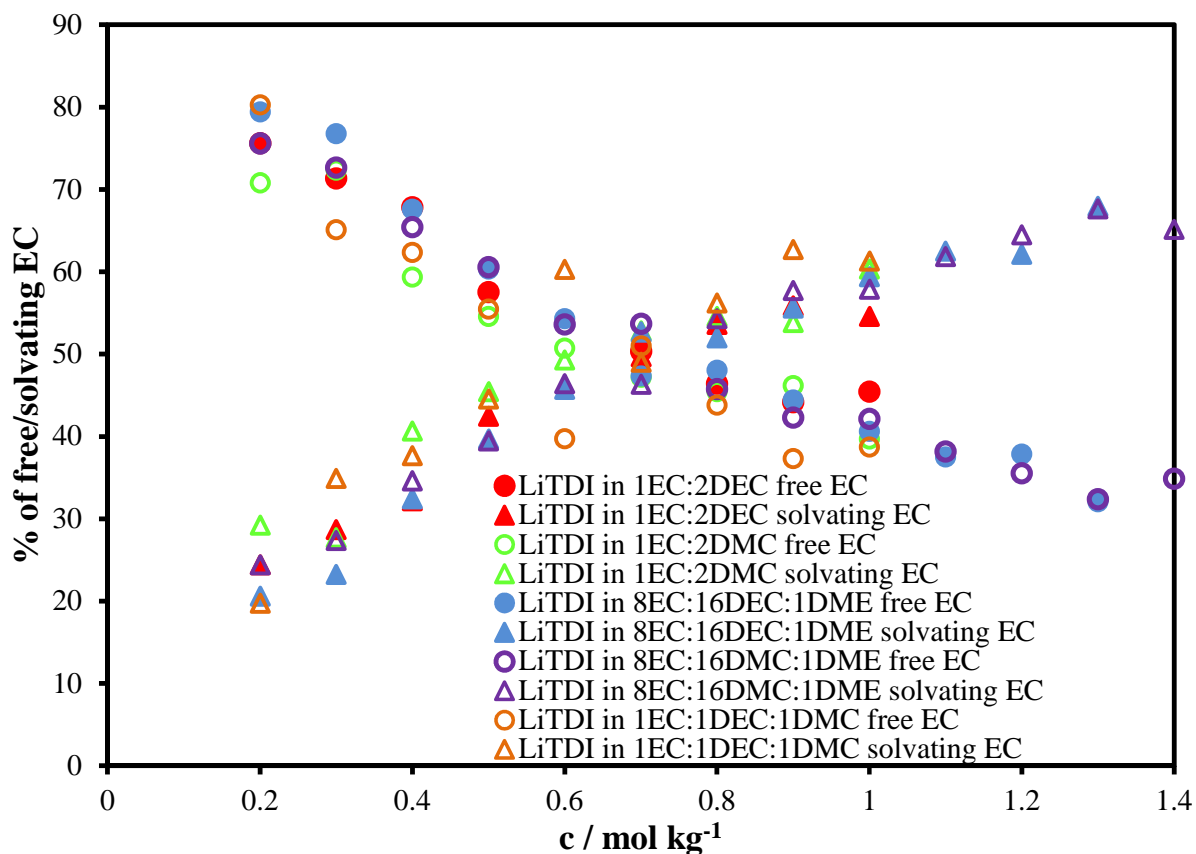
Fig. 4. Ethylene carbonate (EC) distribution as free solvent or solvating molecule dependence of LiTDI concentration in electrolytes.

salt content. It has to be noted that for all solvent mixtures at 0.6-0.8 mol kg^{-1}, the fraction of the "coordinated" solvent begins to dominate over the free solvent. In this concentration range, unusual changes of conductivity (caused by an unusual viscosity curve) can be observed. Viscosity changes in this concentration range can be explained by passing the threshold of solvent fractions involved and uninvolved in the solvation layers of Li$^+$ cation. That, on the other hand, has to be calculated in reference to EC content in solvent mixture, as EC has a dielectric constant far exceeding those of DMC, DEC and DME, thus being the most preferred in a solvation layer. Upon exceeding more or less four EC associated molecules per one lithium cation (at 0.2-0.3 mol kg^{-1}), the conductivity drops. This is because of a lack of a proper solvation layer around the lithium cation, which relies on employing DME or linear carbonate to fill the void created by the lack of EC to coordinate cation. Due to that, lithium cations are more prone to form ionic pairs or dimers with anion(s). This effects conductivity. Another sudden change in conductivity is at about 0.6-0.7 mol kg^{-1}, which corresponds to three EC per one lithium cation ratio. The last conductivity change is caused by the two EC per one lithium cation ratio, at about 1.2-1.3 mol kg^{-1} (depending on the solvent mixture). In

all solvent mixtures, the concentration of the EC is about 3.7 mol kg^{-1} (3.78 for 1EC:2DEC, 1EC:2DMC and 1EC:1DEC:1DMC; 3.64 for 8EC:16DEC:1DME and 8EC:16DMC:1DME). However, not all EC molecules take part in lithium cation solvation – depending on the concentration, the solvating fraction of EC is between 80 and 32%. The compilation of calculated ratios between lithium cations and EC molecules involved in solvation depending on concentration is shown in Table 3. The most interesting points on the conductivity and viscosity plots are overlapped with thresholds of integer values of $EC_{solvating}$:Li. LiTDI solubility limits for mixtures not containing DME are also explained by this ratio – solubility ends as the $EC_{solvating}$:Li value of a given solution approaches 2.

c / mol kg^{-1}	1EC:2DEC	1EC:2DMC	8EC:16DEC:1DME	8EC:16DMC:1DME	1EC:1DEC:1DMC
0.2	4.61	5.52	3.89	4.61	3.73
0.3	3.61	3.49	2.93	3.45	4.40
0.4	3.04	3.84	3.06	3.27	3.56
0.5	3.21	3.44	3.00	2.98	3.37
0.6		3.10	2.88	2.92	3.80
0.7	2.68	2.85	2.85	2.50	2.65
0.8	2.53	2.58	2.45	2.57	2.66
0.9	2.35	2.26	2.33	2.42	2.63
1.0	2.06	2.28	2.25	2.19	2.32
1.1			2.15	2.13	
1.2			1.96	2.03	
1.3			1.98	1.97	
1.4				1.76	

Table 3. Solvated EC molecules to lithium cations ratio dependence of concentration of LiTDI in solvate mixtures (numbers before solvents' names mean their weight ratio values).

The comparison of CN stretching vibration ranges in the IR spectra of the LiTDI-1EC:2DMC electrolytes is shown in Figure 5. It can be seen that the increase of the salt concentration results in a shift of the maximum of the main peak to higher wavenumbers and an increase of the intensity of the broad shoulder at ~2248 cm^{-1}. An exemplary deconvolution of the CN stretching vibration mode of the TDI anion is presented in Figure 6. Although the significant role of the imidazole ring in the formation of ionic associates has been suggested by the theoretical studies of Scheers [23], the significance of the nitrile group in this process is
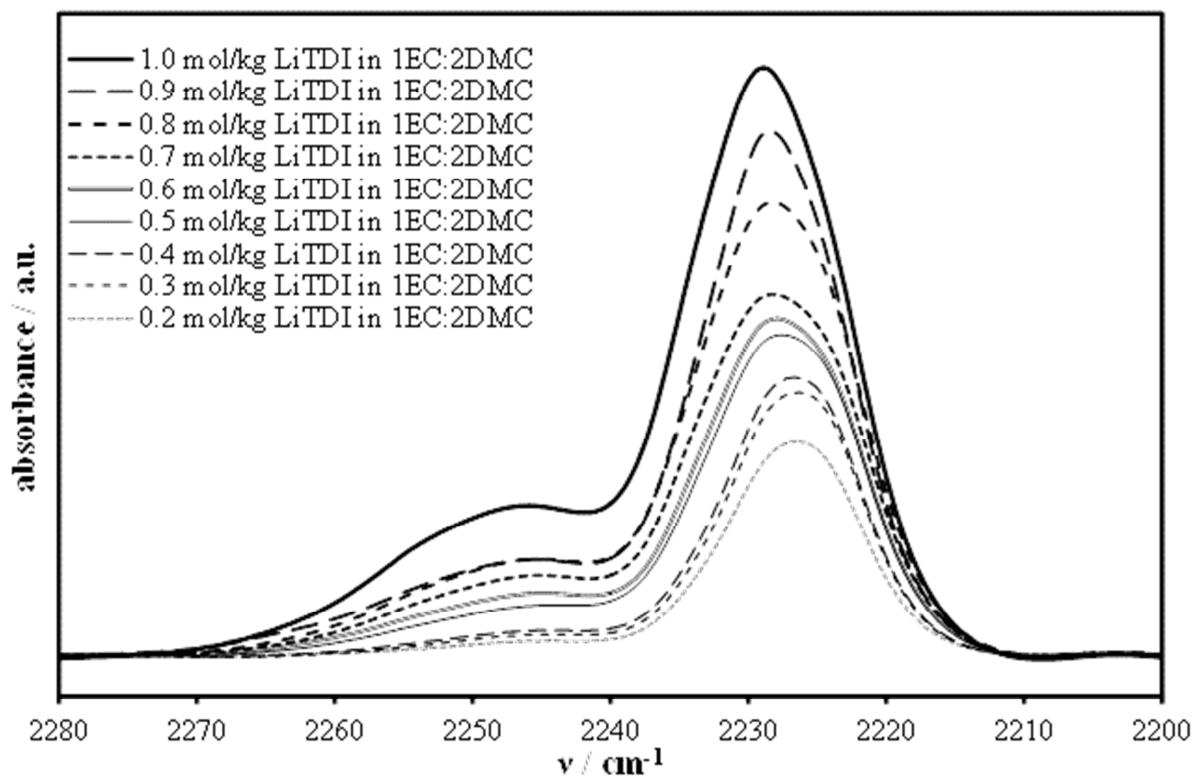
Fig. 5. Comparison of CN stretching band range for different concentration of LiTDI in EC:DMC (1:2 weight ratio) mixtures.
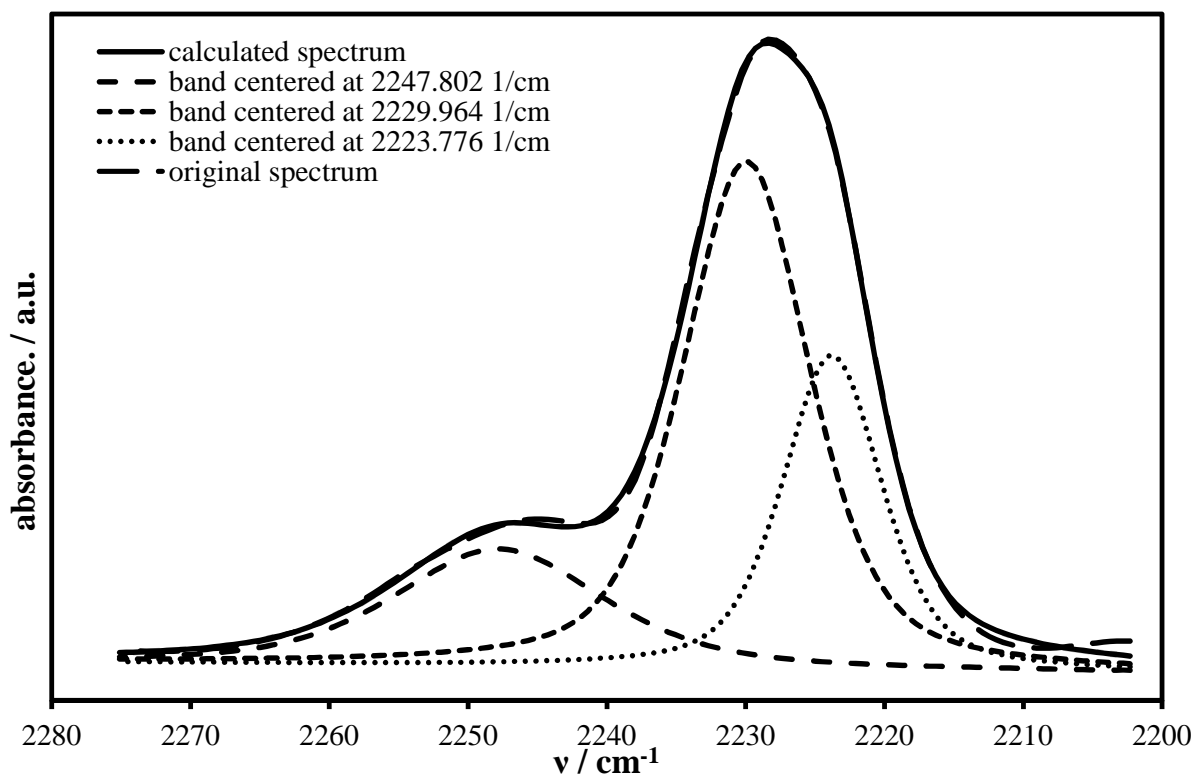

Fig. 6. Example of CN stretching band deconvolution: 0.7 mol kg^{-1} LiTDI in EC-DMC (1:2 weight ratio) mixture, spectrum made in 0.015 mm NaCl window cell.

indicated by structural studies of Dranka et al [24]. A comparison of the Raman spectra of LITDI-acetonitrile solvates with XRD data, made in the latter article, allows for the conclusion that in liquid systems at high salt concentrations, similar species (dimers) must exist. Three bands obtained by the deconvolution of the CN stretching band should correspond to free anions (2223 cm^{-1}), ionic pairs (2229 cm^{-1}) and dimers (2248 cm^{-1}). In the structure of the latter, each TDI anion coordinates two cations, through nitrogen in the aromatic ring and nitrile group at the neighboring carbon. In ionic pairs, lithium can be coordinated by any of the available nitrogen atoms in the TDI structure, but coordination through nitrile seems privileged due to steric reasons.

Dependence of the free anion, ionic pair and dimer fractions obtained from the deconvolution of ν_{CN} in the IR spectra are shown in Figure 7. The share of the free anions decreases and the share of dimers increases with a rise in salt concentration, while for ionic pairs no clear trend was observed, but their share remains on a high level (55- 65%) for all the studied systems. The amount of free anions is higher for DMC containing systems within all concentration ranges around integer-value $EC_{solvating}$:Li thresholds. As the level of ionic pairs is similar in all systems, higher free anion levels are connected to lower levels of dimers, which, as a consequence, has an effect on conductivity, as dimers do not move in the electric field. This overlaps with the higher solvating fraction of EC at the concentration ranges in 1EC:2DMC and 8EC:16DMC:1DME solvent mixtures comparing to other, DEC containing mixtures (Figure 4). Another significant factor for such a difference between DMC- and DEC-containing mixtures is that DMC has both a lower viscosity and a higher dielectric constant than that of DEC [10], so should form better conducting mixtures. As DMC containing systems have indeed higher conductivity and lithium cation conductivity (Table 2), this allows for the conclusion that both EC solvation and the number of EC molecules per lithium cation in the system have a direct impact on electrolyte parameters. As a consequence, electrolyte parameters such as conductivity and lithium cation conductivity can be fine-tuned by composing a proper mixture, including choice of solvent, ratio and salt concentration.
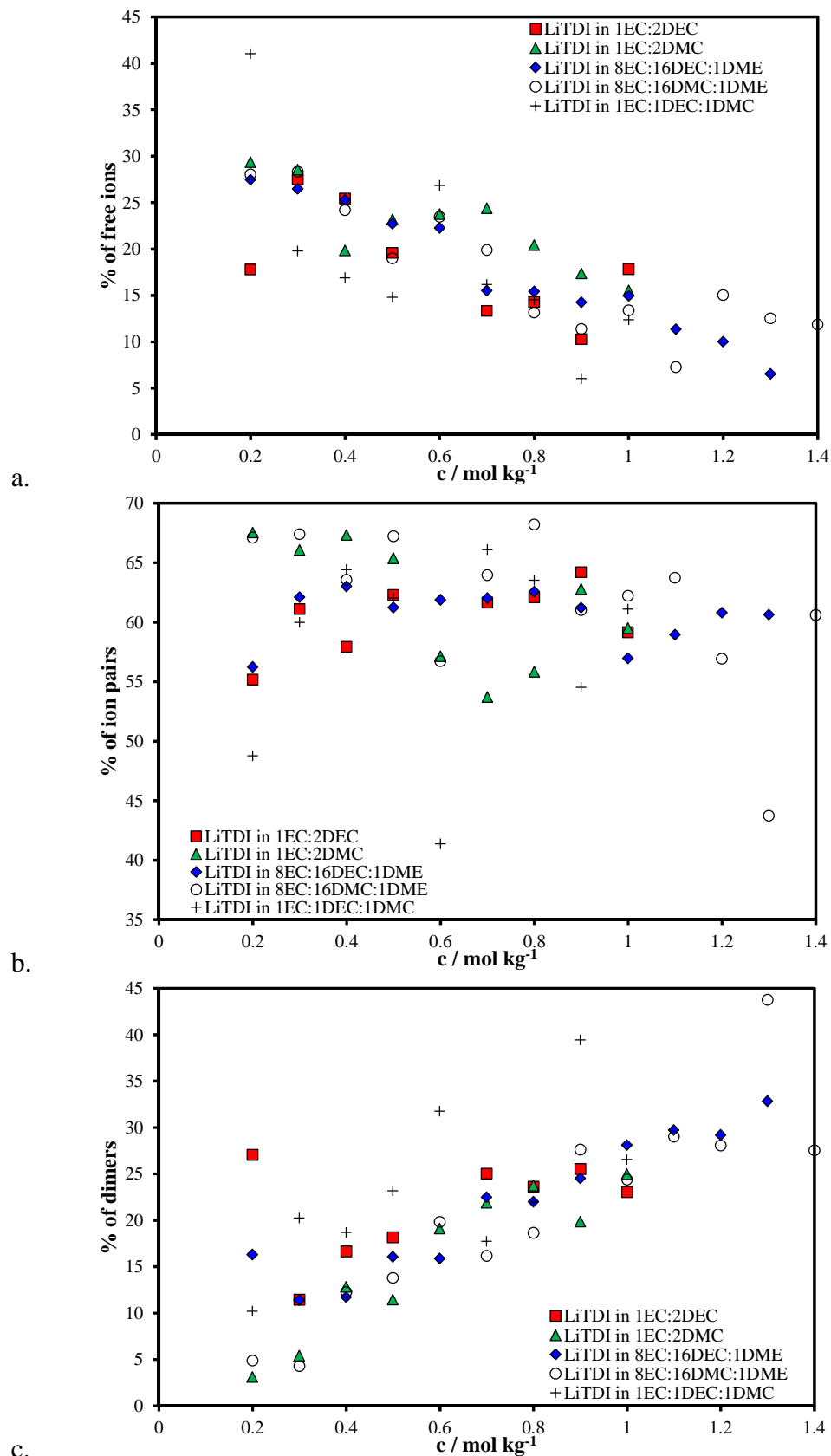
Fig. 7. Electrolyte ionic species fractions calculated from deconvolution of FTIR spectra bands dependence of LiTDI concentration in different electrolytes: a) free ions (solvated); b) ion pairs; c) dimers.

4. Conclusions

New salt, LiTDI, was used for electrolyte optimization in popular battery solvent mixtures, namely: 1EC:2DEC, 1EC:2DMC, 1EC:1DEC:1DMC, 8EC:16DEC:1DME and 8EC:16DMC:1DME. It clearly appeared that LiTDI solutions exhibit substantially different shapes of ionic conductivity vs. salt concentration dependence than observed for other typical lithium salts [8,25]. Electrolytes comprising LiTDI do not show one distinct maximum, but the σ rises gradually, reaching a plateau with a low onset (*e.g.* at 0.31 M for the 1EC:2DMC solution). Also at this point, the σ_{Li+} is high (3.17 mS cm^{-1}) and, more notably, comparable to the industry standard (3.55 mS cm^{-1}), using three times less salt and obtaining a 2.5 times higher transference number, which means a much higher charge-discharge cycle yield. This particular observation indicates the possibility of saving even 2/3 of the salt without sacrificing electrolyte performance in real life applications.

References

[1]   David+Company report: *Lithium Ion Batteries Outlook And Alternative Energy Vehicles (Hevs, Phevs, Evs)-Technologies, Markets, Competitors And Opportunities: 2010-2020 Analysis And Forecasts*, April 4th, 2011.

[2]   Pike Research report: *Lithium Ion Batteries for Hybrid, Plug-in Hybrid, and Battery Electric Vehicles: Market Analysis and Forecasts*, 4Q 2011.

[3]   L. Gaines, R. Cuenca, *Costs of Lithium-Ion Batteries for Vehicles*, Center for Transportation Research Argonne National Laboratory report, May 2000.

[4] C. Cluzel, C. Douglas, *Cost and performance of EV batteries*, Element Energy Limited report for The Committee on Climate Change, March 21st, 2012.

[5] J.B. Goodenough, Y. Kim, Chem. Mater. 22 (2010) 587.

[6] A. Kraytsberg, Y. Ein-Eli, Adv. Energy Mater. 2 (2012) 922.

[7] M.C. Smart, B.V. Ratnakumar, L.D. Whitcanack, K.B. Chin, S. Surampudi, H. Croft, D. Tice, R. Staniewicz, J. Power Sources 119-121 (2003) 349.

[8] M.S. Ding, T.R. Jow, J. Electrochem. Soc. 150 (2003) A620.

[9] L. Niedzicki, G.Z. Żukowska, M. Bukowska, P. Szczeciński, S. Grugeon, S. Laruelle, M. Armand, S. Panero, B. Scrosati, M. Marcinek, W. Wieczorek, Electrochim. Acta 55 (2010) 1450.

[10] K. Xu, Chem. Rev. 104 (2004) 4303.

[11] J.O. Besenhard, M. Winter, J. Yang, W. Biberacher, J. Power Sources 54 (1995) 228.

[12] D. Aurbach, J. Power Sources 119-121 (2003) 497.

[13] M. Wakihara, Mater. Sci. Eng. R Rep. 33 (2001) 109.

[14] K.M. Abraham, J.L. Goldman, D.L. Natwig, J. Electrochem. Soc. 129 (1982) 2404.

[15] L. Niedzicki, M. Kasprzyk, K. Kuziak, G.Z. Żukowska, M. Armand, M. Bukowska, M. Marcinek, P. Szczeciński, W. Wieczorek, J. Power Sources 192 (2009) 612.

[16] L. Niedzicki, S. Grugeon, S. Laruelle, P. Judeinstein, M. Bukowska, J. Prejzner, P. Szczeciński, W. Wieczorek, M. Armand, J. Power Sources 196 (2011) 8696.

[17] M.S. Ding, K. Xu, S. Zhang, T.R. Jow, J. Electrochem. Soc. 148 (2001) A299.

[18] M.S. Ding, J. Electrochem. Soc. 151 (2004) A731.

[19] P. Bruce, C. Vincent, J. Electroanal. Chem. 225 (1987) 1.

[20] Equivalent Circuit, Version 4.55, Copyright by B. A. Boukamp.

[21] C. Kraus, R. Fuoss, J. Am. Chem. Soc. 55 (1933) 21.

[22] J. MacCallum, A. Tomlin, C. Vincent, Eur. Polym. J. 22 (1986) 787.

[23] J. Scheers, L. Niedzicki, G.Z. Żukowska, P. Johansson, W. Wieczorek, P. Jacobsson, Phys. Chem. Chem. Phys. 13 (2011) 11136.

[24] M. Dranka, L. Niedzicki, M. Kasprzyk, M. Marcinek, W. Wieczorek, J. Zachara, Polyhedron 51 (2013) 111.

[25] M.S. Ding, J. Electrochem. Soc. 151 (2004) A40.